

# REGION-TO-REGION KERNEL INTERPOLATION OF ACOUSTIC TRANSFER FUNCTION WITH DIRECTIONAL WEIGHTING

Juliano G. C. Ribeiro, Shoichi Koyama, and Hiroshi Saruwatari

The University of Tokyo, 7-3-1 Hongo, Bunkyo-ku, Tokyo 113-8656, Japan

## ABSTRACT

A method of interpolating the acoustic transfer function (ATF) between regions that takes into account both the physical properties of the ATF and the directionality of region configurations is proposed. Most spatial ATF interpolation methods are limited to estimation in the region of receivers. A kernel method for region-to-region ATF interpolation makes it possible to estimate the ATFs for both source and receiver regions from a discrete set of ATF measurements. We newly formulate the reproducing kernel Hilbert space and associated kernel function incorporating directional weight to enhance the interpolation accuracy. We also investigate hyperparameter optimization methods for this kernel function. Numerical experiments indicate that the proposed method outperforms the method without the use of directional weighting.

**Index Terms**— Acoustic transfer function, Helmholtz equation, kernel ridge regression, directional weighting, hyperparameter optimization.

## 1. INTRODUCTION

The acoustic transfer function (ATF) characterizes sound propagation between two points in an acoustic environment, which is equivalent to the frequency response from a source to a receiver at these points. The ATF estimation of an environment has many applications, such as sound reproduction [1], sound field equalization [2], echo cancellation [3], and speech dereverberation [4].

The spatial interpolation of the ATF is widely studied because of its applicability. The ATF is generally represented as the frequency response of an impulse signal under the assumption of a linear time-invariant system. Thus, one method is to treat the ATF as a rational transfer function with poles/zeros [5,6]. Although the pole locations relative to the receiver position can be predicted, the relation between the locations of poles and/or zeros and the source position cannot. In addition, this method is dependent on the room shape and its eigenmodes. Several attempts have been made to spatially interpolate the ATF based on the sparsity of planewave components [7, 8]. However, those methods are limited to variable receiver positions within a receiver region, with a fixed source.

Sound field estimation or reconstruction is a problem similar to the spatial interpolation of the ATF, and is aimed at estimating the continuous pressure distribution from a discrete set of microphones. Many sound field estimation methods are based on series expansions of finite-dimensional basis functions using planewaves and spherical wavefunctions [9, 10]. An alternative approach is the *kernel method*, where the solution space of the homogeneous Helmholtz equation is defined as the reproducing kernel Hilbert space (RKHS), and the estimate is obtained by kernel ridge regression [11, 12]. This infinite-dimensional analysis of the sound field makes it possible to estimate

it without truncating the expansion order and has been used in various applications, such as spatial audio reproduction [13, 14], active noise cancellation [15], and sensor placement optimization [16].

In a prior work of the authors [17], an ATF interpolation method for both variable source and receiver positions, i.e., *region-to-region ATF interpolation*, based on the kernel method was proposed. The definition of the RKHS is based on acoustic properties of ATFs: the constraint of satisfying the homogeneous Helmholtz equation for the reverberant component and acoustic reciprocity. This method significantly outperformed the method based on a finite-dimensional expansion of spherical wavefunctions proposed in [18].

In this paper, we extend the kernel method of region-to-region ATF interpolation to incorporate directional weight. The directional weight has recently been introduced in the kernel method for sound field estimation to take prior information on source directions into consideration [19, 20]. We introduce the directional weight for the region-to-region ATF interpolation to incorporate knowledge of the configuration of source and receiver regions. Since the use of directional weight requires the determination of several hyperparameters of the reproducing kernel functions, we also investigate hyperparameter optimization methods. Numerical experiments are conducted to compare the proposed method with the method without directional weighting in order to evaluate the effect of directionality on the estimations.

## 2. PROBLEM STATEMENT AND PRELIMINARIES

Given a space  $\Omega \subset \mathbb{R}^3$  with stationary acoustic properties, our objective is to estimate the ATF  $h: \Omega_R \times \Omega_S \rightarrow \mathbb{C}$  between any source/receiver pair of positions  $\mathbf{r} \in \Omega_R \subset \Omega$  and  $\mathbf{s} \in \Omega_S \subset \Omega$ , where  $\Omega_S$  and  $\Omega_R$  are the source and receiver regions, respectively (see Fig. 1).

### 2.1. Preliminaries

We assume that any ATF  $h$  can be separated into two components: a known direct component  $h_D$  given as the free-field Green's function  $G_0$  and an unknown reverberant component  $h_R$ , as shown in [17, 18].  $h_R$  satisfies the homogeneous Helmholtz equation [21]. These assumptions are represented as

$$h(\mathbf{r}|\mathbf{s}, k) = h_D(\mathbf{r}|\mathbf{s}, k) + h_R(\mathbf{r}|\mathbf{s}, k) \quad (1)$$

$$h_D(\mathbf{r}|\mathbf{s}, k) = G_0(\mathbf{r}|\mathbf{s}, k) = \frac{e^{ik\|\mathbf{r}-\mathbf{s}\|}}{4\pi\|\mathbf{r}-\mathbf{s}\|} \quad (2)$$

$$(\nabla_{\mathbf{r}}^2 + k^2)h_R(\mathbf{r}|\mathbf{s}, k) = (\nabla_{\mathbf{s}}^2 + k^2)h_R(\mathbf{r}|\mathbf{s}, k) = 0, \quad (3)$$

where  $\mathbf{r}|\mathbf{s}$  is the source/receiver pair of positions,  $i$  is the imaginary unit,  $\nabla_{\mathbf{r}}^2$  and  $\nabla_{\mathbf{s}}^2$  are the Laplacian operators on the coordinates of

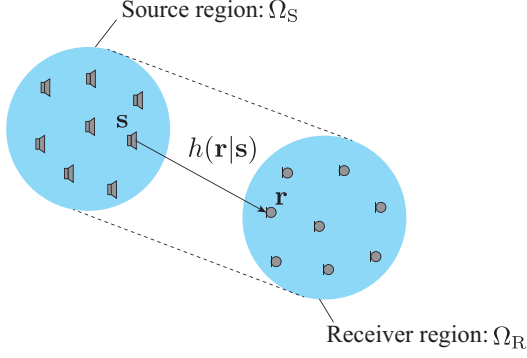


**Fig. 1:** Schematic diagram of a region-to-region ATF interpolation problem.

$\mathbf{r}$  and  $\mathbf{s}$ , respectively,  $k = 2\pi\tilde{f}/c$  is the wavenumber,  $\tilde{f}$  is the frequency, and  $c$  is the speed of sound. Hereafter,  $k$  in the argument of the ATFs is omitted for notational simplicity.

## 2.2. Region-to-region ATF interpolation problem

We distribute a set of  $M$  receivers at points  $\{\mathbf{r}_m\}_{m=1}^M$  and  $L$  sources at points  $\{\mathbf{s}_l\}_{l=1}^L$  to obtain a total of  $N (= LM)$  ATF measurement values. We collectively denote  $\mathbf{q}_n = \mathbf{r}_m|\mathbf{s}_l$  for the position pairs with index  $n = m + (l-1)M (\in \{1, \dots, N\})$ . A set of  $N$  ATFs is given, and then the direct component is removed from them to obtain the measurement vector  $\mathbf{y} = [y_1, \dots, y_N]^T$  corresponding to each  $\mathbf{q}_n$ . We define our optimization problem as

$$\begin{aligned} \hat{h}_R &= \arg \min_{f \in \mathcal{H}} \mathcal{J}(f) \\ \mathcal{J}(f) &:= \sum_{n=1}^N |y_n - f(\mathbf{q}_n)|^2 + \lambda \|f\|_{\mathcal{H}}^2, \quad f \in \mathcal{H}, \end{aligned} \quad (4)$$

where  $\lambda > 0$  is the regularization constant and  $\mathcal{H}$  is the feature space to which the interpolation of the reverberant component belongs. This interpolation function is then added to the direct component to obtain  $\hat{h}$ :

$$\hat{h}(\mathbf{r}|\mathbf{s}) = h_D(\mathbf{r}|\mathbf{s}) + \hat{h}_R(\mathbf{r}|\mathbf{s}). \quad (5)$$

## 2.3. Kernel ridge regression

We consider the space  $\mathcal{H}$  to be a reproducing kernel Hilbert space (RKHS). That is, it is a Hilbert space  $(\mathcal{H}, \langle \cdot, \cdot \rangle_{\mathcal{H}})$  that admits a reproducing kernel function  $\kappa$ . The reproducing kernel is a bivariate function that satisfies:

$$\langle \kappa(\cdot, \mathbf{r}|\mathbf{s}), f \rangle_{\mathcal{H}} = f(\mathbf{r}|\mathbf{s}), \quad \forall \mathbf{r} \in \Omega_R, \quad \forall \mathbf{s} \in \Omega_S. \quad (6)$$

In that case, the interpolation function  $\hat{h}_R$  is given by kernel ridge regression:

$$\hat{h}_R(\mathbf{r}|\mathbf{s}) = \kappa(\mathbf{r}|\mathbf{s})(\mathbf{K} + \lambda\mathbf{I})^{-1}\mathbf{y}, \quad (7)$$

where  $\kappa(\mathbf{r}|\mathbf{s}) = [\kappa(\mathbf{r}|\mathbf{s}, \mathbf{q}_1), \dots, \kappa(\mathbf{r}|\mathbf{s}, \mathbf{q}_N)]$  is the kernel function vector,  $\mathbf{I}$  is the identity matrix, and  $\mathbf{K}$  is the Gram matrix defined as

$$\mathbf{K} = \begin{bmatrix} \kappa(\mathbf{q}_1, \mathbf{q}_1) & \kappa(\mathbf{q}_1, \mathbf{q}_2) & \dots & \kappa(\mathbf{q}_1, \mathbf{q}_N) \\ \vdots & \vdots & \ddots & \vdots \\ \kappa(\mathbf{q}_N, \mathbf{q}_1) & \kappa(\mathbf{q}_N, \mathbf{q}_2) & \dots & \kappa(\mathbf{q}_N, \mathbf{q}_N) \end{bmatrix}. \quad (8)$$

## 3. REGION-TO-REGION ATF INTERPOLATION WITH DIRECTIONAL WEIGHTING

We previously formulated an RKHS for solving (4) based on the spherical wavefunction expansion in a previous study [17]. We now formulate an RKHS based on the planewave expansion incorporating directional weight to take into consideration the behavior of the ATF with respect to the relative positions of  $\Omega_R$  and  $\Omega_S$ .

### 3.1. Feature space definition

Since the reverberant component  $h_R$  does not include any sources in  $\Omega_S$  and  $\Omega_R$ ,  $h_R$  can be represented by a planewave expansion, i.e., *Herglotz wavefunction* [22], as

$$h_R(\mathbf{r}|\mathbf{s}) = \mathcal{I}(\tilde{h}_R; \mathbf{r}|\mathbf{s}), \quad (9)$$

$$\mathcal{I}(f; \mathbf{r}|\mathbf{s}) := \int_{\mathbb{S}^2 \times \mathbb{S}^2} e^{ik(\hat{\mathbf{r}} \cdot \mathbf{r} + \hat{\mathbf{s}} \cdot \mathbf{s})} f(\hat{\mathbf{r}}, \hat{\mathbf{s}}) d\hat{\mathbf{r}} d\hat{\mathbf{s}}, \quad (10)$$

where  $\mathcal{I}$  is the operator for the planewave expansion, and  $\mathbb{S}^2$  is the set of vectors in  $\mathbb{R}^3$  of unit norm, representing directions. Therefore,  $\tilde{h}_R(\hat{\mathbf{r}}, \hat{\mathbf{s}})$  is the complex amplitude of the planewave component of  $h_R$  from the source direction  $\hat{\mathbf{s}}$  to the receiver direction  $\hat{\mathbf{r}}$ . The reciprocity of  $h_R$  imposes the condition that  $\tilde{h}_R(\hat{\mathbf{r}}, \hat{\mathbf{s}}) = \tilde{h}_R(\hat{\mathbf{s}}, \hat{\mathbf{r}})$ . Thus, our inner-product space  $(\mathcal{H}, \langle \cdot, \cdot \rangle_{\mathcal{H}})$  is defined as

$$\begin{aligned} \mathcal{H} &= \left\{ h_R = \mathcal{I}(\tilde{h}_R; \mathbf{r}|\mathbf{s}) : \tilde{h}_R \in L^2(W, \mathbb{S}^2 \times \mathbb{S}^2), \right. \\ &\quad \left. \tilde{h}_R(\hat{\mathbf{r}}, \hat{\mathbf{s}}) = \tilde{h}_R(\hat{\mathbf{s}}, \hat{\mathbf{r}}) \quad \forall \hat{\mathbf{r}}, \hat{\mathbf{s}} \in \mathbb{S}^2 \right\} \end{aligned} \quad (11)$$

$$\langle f, g \rangle_{\mathcal{H}} = \int_{\mathbb{S}^2 \times \mathbb{S}^2} \frac{\overline{\tilde{f}(\hat{\mathbf{r}}, \hat{\mathbf{s}})} \tilde{g}(\hat{\mathbf{r}}, \hat{\mathbf{s}})}{W(\hat{\mathbf{r}}, \hat{\mathbf{s}})} d\hat{\mathbf{r}} d\hat{\mathbf{s}}, \quad \forall f, g \in \mathcal{H}, \quad (12)$$

where  $\overline{\cdot}$  is the complex conjugate,  $W: \mathbb{S}^2 \times \mathbb{S}^2 \rightarrow \mathbb{R}_+$  is a directional weighting function, and  $L^2(W, \mathbb{S}^2 \times \mathbb{S}^2)$  is the space of functions of bounded square integral for  $W$ . Under these conditions,  $(\mathcal{H}, \langle \cdot, \cdot \rangle_{\mathcal{H}})$  inherits the completeness of  $L^2$  spaces [23] and as such is a Hilbert space. We can show that it is an RKHS by showing that the following function is its reproducing kernel:

To show that this function is the reproducing kernel, we only have to show that it satisfies the projection property for any given  $f \in \mathcal{H}$ :

$$\begin{aligned} \langle \kappa(\cdot, \mathbf{r}|\mathbf{s}), f \rangle_{\mathcal{H}} &= \int_{\mathbb{S}^2 \times \mathbb{S}^2} \frac{e^{ik(\hat{\mathbf{r}} \cdot \mathbf{r} + \hat{\mathbf{s}} \cdot \mathbf{s})} \tilde{f} + e^{ik(\hat{\mathbf{r}} \cdot \mathbf{s} + \hat{\mathbf{s}} \cdot \mathbf{r})} \tilde{f}}{2} d\hat{\mathbf{r}} d\hat{\mathbf{s}} \\ &= \frac{1}{2} \left( \mathcal{I}(\tilde{f}; \mathbf{r}|\mathbf{s}) + \mathcal{I}(\tilde{f}; \mathbf{s}|\mathbf{r}) \right) \\ &= \frac{f(\mathbf{r}|\mathbf{s}) + f(\mathbf{s}|\mathbf{r})}{2}. \end{aligned} \quad (13)$$

Since  $f$  is reciprocal, we have

$$\langle \kappa(\cdot, \mathbf{r}|\mathbf{s}), f \rangle_{\mathcal{H}} = f(\mathbf{r}|\mathbf{s}). \quad (14)$$

We also consider that the directional weighting function  $W$  is separable for  $\hat{\mathbf{r}}$  and  $\hat{\mathbf{s}}$ , that is,

$$W(\hat{\mathbf{r}}, \hat{\mathbf{s}}) = w(\hat{\mathbf{r}})w(\hat{\mathbf{s}}), \quad (15)$$

where  $w: \mathbb{S}^2 \rightarrow \mathbb{R}_+$  is a directional weighting function in a single direction.

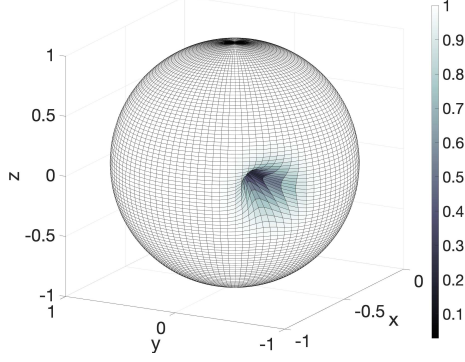


**Fig. 2:** Directional weighting function  $w$  when  $\hat{\mathbf{v}}_0 = [-1/\sqrt{2}, -1/\sqrt{2}, 0]^T$ ,  $\gamma = 0.01$ , and  $\beta = 100$ . The gain is given by the distance from the origin to the surface, quantified according to the bar on the right.

### 3.2. Proposed directional weighting function

Since the direct component is removed from the measurements to obtain the reverberant component, the directional weighting function for the region-to-region ATF interpolation should have minimal gain in the direction connecting the centers of both regions, which is defined as  $\hat{\mathbf{v}}_0$ . Therefore, we define the directional weighting function  $w$  as

$$w(\hat{\mathbf{v}}) = \frac{1}{4\pi} \left( 1 + \gamma^2 - \frac{\cosh(\beta \hat{\mathbf{v}} \cdot \hat{\mathbf{v}}_0)}{\cosh(\beta)} \right), \quad \hat{\mathbf{v}} \in \mathbb{S}^2. \quad (16)$$

The hyperparameters  $\beta$  and  $\gamma$  characterize  $\Omega$  acoustically. Since the direct components are expected to be weaker, the early reflections are expected to be significantly more influential. An increase in  $\beta$  makes the weight more selective in regards to the lateral components, while  $\gamma$  sets the minimum gain baseline for all directions.

To better illustrate this, an example of the directional weighting function is plotted in Fig. 2, which shows that the weight is minimal in the chosen direction  $\hat{\mathbf{v}}_0$  but maximal in the lateral directions.  $\beta$  controls the width of the cavity passing through  $\hat{\mathbf{v}}_0$ , while  $\gamma$  controls the depth.

### 3.3. Relation to prior work using uniform weight

By setting  $\gamma = 1$  and  $\beta = 0$ , the directional weighting function becomes uniform, i.e.,  $w = 1/4\pi$ . The reproducing kernel of this uniform weight has the closed form

$$\kappa(\mathbf{r}|\mathbf{s}, \mathbf{r}'|\mathbf{s}') = \frac{1}{2} \left( j_0(k\|\mathbf{r} - \mathbf{r}'\|)j_0(k\|\mathbf{s} - \mathbf{s}'\|) + j_0(k\|\mathbf{s} - \mathbf{r}'\|)j_0(k\|\mathbf{r} - \mathbf{s}'\|) \right), \quad (17)$$

where  $j_0$  is the 0th-order spherical Bessel function of the first kind. This kernel function is identical to that used in [17], making both estimations equivalent.

## 4. HYPERPARAMETER OPTIMIZATION FOR DIRECTIONAL WEIGHT

The introduction of hyperparameters in (16) also necessitates a criterion for choosing them. Although the profile of the reverberant component is understood, the exact balance between the direct and lateral component gains is not known outright. There are several

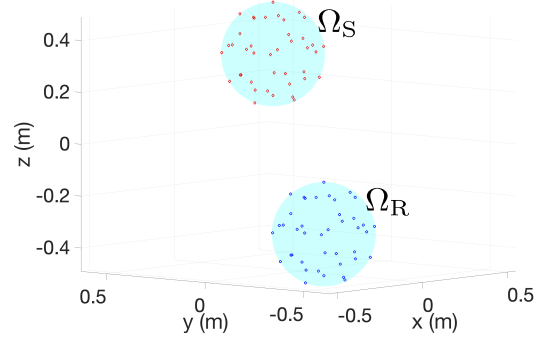


**Fig. 3:** Experimental setup utilized for the simulations. Red diamonds represent sources and blue circles represent receivers.

methods of hyperparameter optimization used for kernel ridge regression [24, 25]. For this application, we employ leave-one-out cross-validation (LOO) because of its simplicity and nearly unbiased nature [26].

We begin the computation of LOO by selecting a data point and measurement point pair  $(\mathbf{q}_n, y_n)$  to remove from the data set. We then derive the desired model using the remaining  $N - 1$  elements of the data set and compute the error in estimating  $y_n$  with this partial model. The value of LOO is the average of all errors calculated by repeating this process exhaustively:

$$\text{LOO}(\mathbf{y}, \ell) = \frac{1}{N} \sum_{n=1}^N \ell(\hat{f}_n(\mathbf{q}_n) - y_n), \quad (18)$$

where  $\ell$  is the chosen loss function, and  $\hat{f}_n$  is the model derived when considering all data pairs except  $(\mathbf{q}_n, y_n)$ . We consider two types of loss function  $\ell$ : square error (SQE) and Tukey loss.

$$\text{SQE}(z) = |z|^2 \quad (19)$$

$$\text{Tukey}(z) = \begin{cases} \frac{\sigma^2}{6} \left( 1 - \left( 1 - \frac{|z|^2}{\sigma^2} \right)^3 \right), & |z| \leq \sigma \\ \frac{\sigma^2}{6}, & |z| > \sigma \end{cases}, \quad (20)$$

where  $z$  is a complex variable, and  $\sigma$  is the selectivity parameter. Tukey loss is more selective than SQE, which means that these loss functions have similar behavior near 0, but Tukey loss has slower growth for higher discrepancies. This selectivity makes Tukey loss more resilient to outliers.

Both SQE and Tukey loss are differentiable with respect to the hyperparameters, meaning that LOO can be optimized using gradient descent methods. We applied the improved robust back-propagation algorithm introduced in [27].

## 5. NUMERICAL SIMULATIONS

The proposed method using directional weight was evaluated using 3D acoustic simulations based on the image source method [28] by comparing it with the method using uniform weight. The room used for the evaluation was shoebox-shaped and had  $3.2 \text{ m} \times 4.0 \text{ m} \times 2.7 \text{ m}$  dimensions. The reflection coefficients of the walls were set so that the reverberation time  $T_{60}$  was 0.45 s. The source and receiver regions were spheres of 0.2 m radius whose centers were  $\mathbf{s}_0 = [0.35, 0.43, 0.29]^T \text{ m}$  for  $\Omega_S$  and  $\mathbf{r}_0 = -\mathbf{s}_0$  for  $\Omega_R$ . The origin of the coordinate system was set at the center of the room. We used  $\hat{\mathbf{v}}_0 = (\mathbf{r}_0 - \mathbf{s}_0)/\|\mathbf{r}_0 - \mathbf{s}_0\|$  for the directional kernel.

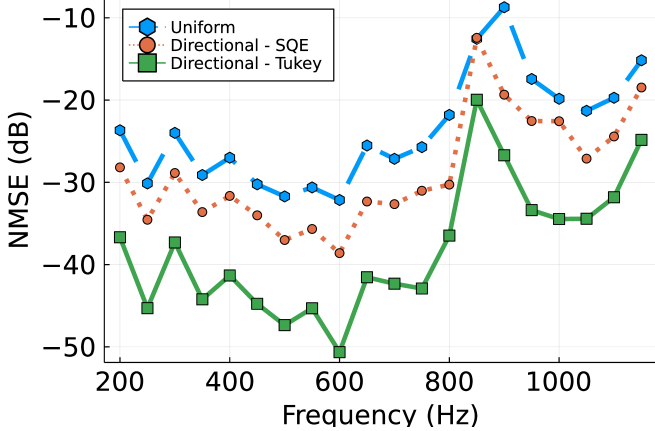


Fig. 4: NMSE performance of the methods compared.

The measurement points were given for a total of  $L = M = 41$  points distributed on two spherical layers. The point distribution was given by the spherical  $t$ -design [29]:  $t = 4$  for the outer layer and  $t = 3$  for the inner layer. We also added Gaussian noise so that the signal-to-noise ratio was 20 dB. The parameter  $\sigma$  in the Tukey loss (20) was set to 0.4, which was determined so that the probability of the error falling within four standard deviations was above 99%. The regularization parameter  $\lambda$  in (7) was set to  $10^{-2}$ .

The evaluation measure was defined as the normalized mean square error (NMSE),

$$\text{NMSE} = 10 \log_{10} \left( \frac{\sum_n |\hat{h}(\mathbf{q}'_n) - h(\mathbf{q}'_n)|^2}{\sum_n |h(\mathbf{q}'_n)|^2} \right), \quad (21)$$

where  $\mathbf{q}'_n$  denote the  $n$ th evaluation source/receiver pair. We set 9025 source/receiver pairs of evaluation.

The NMSE with respect to the frequency ranging from 100 to 1150 Hz is shown in Fig. 4. We also show the estimated ATF in  $\Omega_R$  generated by a single source point at  $[0.35, 0.43, 0.29]^T$  m for 950 Hz in Fig. 5. The normalized squared error distribution of this plot is also shown in Fig. 6, which is defined as

$$\text{NSE}(\mathbf{r}) = 10 \log_{10} \left( \frac{|h(\mathbf{r}|\mathbf{s}_0) - \hat{h}(\mathbf{r}|\mathbf{s}_0)|^2}{|h(\mathbf{r}|\mathbf{s}_0)|^2} \right). \quad (22)$$

The proposed method using directionally weighted kernels achieved a lower NMSE than the uniform counterpart for every frequency. For the SNR of 20 dB, the more selective Tukey loss also significantly outperformed the simpler SQE used in LOO. These results indicate that the directional weight is effective for the region-to-region ATF interpolation problem. In addition, LOO with Tukey loss is more useful for hyperparameter optimization than the simple SQE loss.

## 6. CONCLUSION

We proposed a kernel interpolation method for region-to-region ATF interpolation with directional weighting. The reproducing kernel Hilbert space and associated reproducing kernel function are formulated on the basis of planewave decomposition, having properties of the Helmholtz equation constraint, acoustic reciprocity, and directionality. The spatial interpolation of the ATF is achieved by

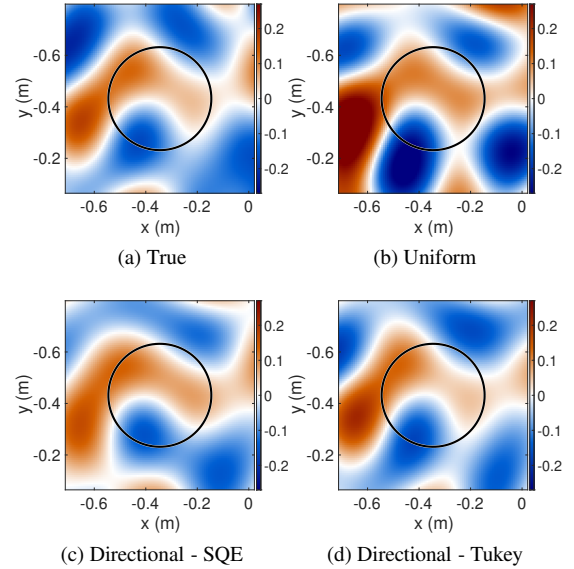


Fig. 5: Distributions of true and estimated ATFs in  $\Omega_R$  from the center of  $\Omega_S$  at  $[0.35, 0.43, 0.29]^T$  m for 950 Hz. The black circle indicates the bounds of  $\Omega_R$ .

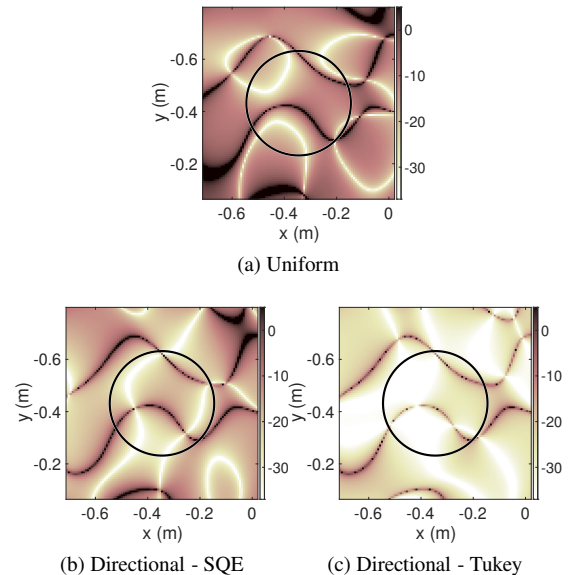


Fig. 6: Distributions of NSEs in  $\Omega_R$ .

kernel ridge regression using this kernel function. Hyperparameters included in the kernel function are optimized by leave-one-out cross-validation. In the numerical experiments, the proposed method achieved highly accurate interpolation compared with the method using uniform weight. Furthermore, robustness to the noise was significantly improved by using Tukey loss in LOO.

## 7. ACKNOWLEDGEMENTS

This work was supported by JSPS KAKENHI Grant Number JP19H01116 and JST PRESTO Grant Number JPMJPR18J4.

## 8. REFERENCES

- [1] F. Borra, I. D. Gebru, and D. Markovic, "Soundfield reconstruction in reverberant environments using higher-order microphones and impulse response measurements," in *Proc. IEEE Int. Conf. Acoust., Speech, Signal Process. (ICASSP)*, 2019, pp. 281–285.
- [2] R. Mazur, F. Katzberg, and A. Mertins, "Robust room equalization using sparse sound-field reconstruction," in *Proc. IEEE Int. Conf. Acoust., Speech, Signal Process. (ICASSP)*, 2019, pp. 4230–4234.
- [3] P. Gil-Cacho, T. van Waterschoot, M. Moonen, and S. Jensen, "Multi-microphone acoustic echo cancellation using multi-channel warped linear prediction of common acoustical poles," in *Proc. European Signal Process. Conf. (EUSIPCO)*, 2010, vol. 2010, pp. 2121–2125.
- [4] N. Mohanan, R. Velmurugan, and P. Rao, "Speech dereverberation using NMF with regularized room impulse response," in *Proc. IEEE Int. Conf. Acoust., Speech, Signal Process. (ICASSP)*, 2017, pp. 4955–4959.
- [5] Y. Haneda, S. Makino, Y. Kaneda, and N. Koizumi, "ARMA modeling of a room transfer function at low frequencies," *J. Acoust. Soc. Jpn. (E)*, vol. 15, pp. 353–355, 1994.
- [6] Y. Haneda, Y. Kaneda, and N. Kitawaki, "Common-acoustical-pole and residue model and its application to spatial interpolation and extrapolation of a room transfer function," *IEEE Trans. Speech Audio Process.*, vol. 7, no. 6, pp. 709–717, 1999.
- [7] R. Mignot, G. Chardon, and L. Daudet, "Low frequency interpolation of room impulse responses using compressed sensing," *IEEE/ACM Trans. Audio, Speech, Lang. Process.*, vol. 22, no. 1, pp. 205–216, 2014.
- [8] N. Antonello, E. De Sena, M. Moonen, P. A. Naylor, and T. van Waterschoot, "Room impulse response interpolation using a sparse spatio-temporal representation of the sound field," *IEEE/ACM Trans. Audio, Speech, Lang. Process.*, vol. 25, no. 10, pp. 1929–1941, 2017.
- [9] M. A. Poletti, "Three-dimensional surround sound systems based on spherical harmonics," *J. Audio Eng. Soc.*, vol. 53, no. 11, pp. 1004–1025, 2005.
- [10] S. Koyama, K. Furuya, Y. Hiwasaki, and Y. Haneda, "Analytical approach to wave field reconstruction filtering in spatio-temporal frequency domain," *IEEE Trans. Audio, Speech, Lang. Process.*, vol. 21, no. 4, pp. 685–696, 2013.
- [11] N. Ueno, S. Koyama, and H. Saruwatari, "Kernel ridge regression with constraint of Helmholtz equation for sound field interpolation," in *Proc. Int. Workshop Acoust. Signal Enhancement (IWAENC)*, 2018, pp. 436–440.
- [12] N. Ueno, S. Koyama, and H. Saruwatari, "Sound field recording using distributed microphones based on harmonic analysis of infinite order," *IEEE Signal Process. Lett.*, vol. 25, no. 1, pp. 135–139, 2018.
- [13] N. Iijima, S. Koyama, and H. Saruwatari, "Binaural rendering from microphone array signals of arbitrary geometry," *J. Acoust. Soc. Am.*, 2021, (in press).
- [14] S. Koyama, K. Kimura, and N. Ueno, "Sound field reproduction with weighted mode matching and infinite-dimensional harmonic analysis: An experimental evaluation," in *Proc. International Conference on Immersive and 3D Audio (I3DA)*, 2021.
- [15] S. Koyama, J. Brunnström, H. Ito, N. Ueno, and H. Saruwatari, "Spatial active noise control based on kernel interpolation of sound field," *IEEE/ACM Trans. Audio, Speech, Lang. Process.*, 2021, (in press).
- [16] K. Ariga, T. Nishida, S. Koyama, N. Ueno, and H. Saruwatari, "Mutual-information-based sensor placement for spatial sound field recording," in *Proc. IEEE Int. Conf. Acoust., Speech, Signal Process. (ICASSP)*, 2020, pp. 166–170.
- [17] J. G. C. Ribeiro, N. Ueno, S. Koyama, and H. Saruwatari, "Kernel interpolation of acoustic transfer function between regions considering reciprocity," in *IEEE Sensor Array Multichannel Signal Process. Workshop (SAM)*, 2020, pp. 1–5.
- [18] P. N. Samarasinghe, T. D. Abhayapala, M. A. Poletti, and T. Betlehem, "An efficient parameterization of the room transfer function," *IEEE/ACM Trans. Audio, Speech, Lang. Process.*, vol. 23, no. 12, pp. 2217–2227, 2015.
- [19] H. Ito, S. Koyama, N. Ueno, and H. Saruwatari, "Spatial active noise control based on kernel interpolation with directional weighting," in *Proc. IEEE Int. Conf. Acoust., Speech, Signal Process. (ICASSP)*, 2020, pp. 8399–8403.
- [20] N. Ueno, S. Koyama, and H. Saruwatari, "Directionally weighted wave field estimation exploiting prior information on source direction," *IEEE Trans. Signal Process.*, vol. 69, pp. 2383–2395, 2021.
- [21] E. G. Williams, *Fourier Acoustics*, Academic Press, London, 1999.
- [22] D. Colton and P. Monk, *Herglotz Wave Functions in Inverse Electromagnetic Scattering Theory*, pp. 367–394, Springer Berlin Heidelberg, Berlin, Heidelberg, 2003.
- [23] W. Rudin, *Functional Analysis*, McGraw-Hill, New York City, 1991.
- [24] R. Horiuchi, S. Koyama, J. G. C. Ribeiro, N. Ueno, and H. Saruwatari, "Kernel learning for sound field estimation with l1 and l2 regularizations," in *Proc. IEEE Int. Workshop Appl. Signal Process. Audio Acoust. (WASPAA)*, 2021 (to appear).
- [25] D. Caviades Nozal, N. Riis, F. Heuchel, J. Brunskog, P. Gerstoft, and E. Fernandez-Grande, "Gaussian processes for sound field reconstruction," *J. Acoust. Soc. Am.*, vol. 149, pp. 1107–1119, 2021.
- [26] A. Elisseeff and M. Pontil, "Leave-one-out error and stability of learning algorithms with applications," *NATO Sci. Ser., III: Comput. Systems Sci.*, vol. 190, pp. 111–130, 2003.
- [27] A. Anastasiadis, G. Magoulas, and M. Vrahatis, "An efficient improvement of the Rprop algorithm," in *Proc. Int. Workshop Artificial Neural Netw. Pattern Recognit. (ANNPR)*, 2003.
- [28] J. B. Allen and D. A. Berkley, "Image method for efficiently simulating small-room acoustics," *J. Acoust. Soc. Am.*, vol. 65, no. 4, pp. 943–950, 1979.
- [29] X. Chen and R. Womersley, "Spherical t-design with  $d=(t+1)^2$  points," (Accessed on Oct. 26, 2018). [Online]. Available: <http://www.polyu.edu.hk/ama/staff/xjchen/sphdesigns.html>.